

COMPARATIVE STUDY OF LOW BETA MULTI-GAP SUPERCONDUCTING BUNCHERS

K. Taletskiy, M. Gusarova¹, MEPhI National Research Nuclear University,
 115409 Moscow, Russia

W. A. Barth^{2,3}, S. Yaramyshev³, GSI Helmholtzzentrum für Schwerionenforschung GmbH,
 64291 Darmstadt, Germany

M. Miski-Oglu, HIM Helmholtz Institute Mainz, 55099 Mainz, Germany

M. Busch, M. Basten, IAP University of Frankfurt, 60438 Frankfurt am Main, Germany

¹also Joint Institute for Nuclear Research, Dubna, Russia

²also HIM Helmholtz Institute Mainz, 55099 Mainz, Germany

³also MEPhI National Research Nuclear University, 115409 Moscow, Russia

Abstract

The results of a comparative study of low beta multi-gap superconducting bunchers for 216.816 MHz and a relative velocity of 0.07c with dedicated limitations of the overall geometrical dimensions are presented. A comparison of electrodynamic, mechanical and thermal properties of 3-gap and 2-gap cavities is shown.

INTRODUCTION

The high current heavy ion accelerator UNILAC (Universal Linear ACcelerator) is currently being upgraded in order to be used as an injector for the FAIR (Facility for Antiproton and Ion Research) project [1-5]. In future the UNILAC will provide high-intensity short pulses [6], while the UNILAC-user program, as the super heavy elements (SHE) research, preferably operates in CW-mode. For that purposes a collaboration of GSI Helmholtzzentrum fuer Schwerionenforschung (GSI, Darmstadt, Germany), Helmholtz Institute Mainz (HIM, Mainz, Germany) and Institut für Angewandte Physik/Goethe-Universität (IAP, Frankfurt am Main, Germany) is currently developing a new superconducting CW-linac [7-11]. High efficiency and compactness of the new machine is ensured by the already achieved high accelerating gradient of 9.6 MV/m with corresponding electric and magnetic peak fields of 60 MV/m and 55 mT respectively [7].

The new linac is designed as a modular structure [12]. The proposed beam dynamics concept assumes the use of Crossbar H-Mode (CH) cavities in combination with two superconducting solenoids and a re-buncher cavity within one cryomodule (Fig. 1).



Figure 1: Proposed layout of the first CW-linac cryomodule comprising 3 CH-DTLs (CH0, CH1 and CH2), S – solenoid and B – re-buncher cavity.

The necessity for fitting the re-buncher into the existing cryostat, together with the already fabricated CH0, CH1 and CH2 cavities, determines the operating frequency (216.816 MHz) of the re-buncher cavity and dictate several constraints on its overall geometrical dimensions (Table 1).

Table 1: Essential Requirements for the New Re-buncher of the New CW-Linac

| Parameter | Designation | Value |
|-------------------|-------------|-----------------|
| Frequency | f , MHz | 216.816 |
| Beam velocity | B | 0.07 |
| Number of gaps | N_g | from 2 to 3 |
| Aperture diameter | D_a , mm | from 30 to 35 |
| Cavity length | L , mm | less than 300 |
| Cavity diameter | D_c , mm | from 410 to 500 |

Therefore, this paper focuses on the comparison of properties of the SC 3-gap and the 2-gap Spoke re-buncher [13], both developed with respect to parameters listed in Table 1.

RF DESIGN

The main challenges of RF optimization were the frequency tuning of the cavity, as well as the lowering of the surface electric and magnetic peak fields down to 30 MV/m and 40 mT respectively [14]. Obviously, this should be performed under the given restrictions for the main cavity dimensions. Geometrical parameters, used for the optimization process, are marked in Fig. 2.

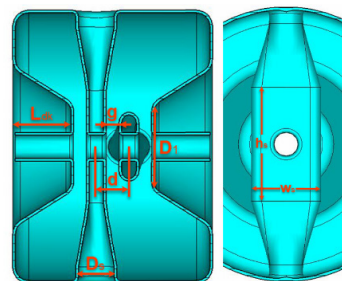


Figure 2: Schematic layout of the 3-gap Spoke cavity with its main dimensions used for RF optimization.

The surface electric and magnetic field distributions in the optimized 3-gap cavity (Fig. 3) do not exceed 30 MV/m (design accelerating gradient is 5.1 MV/m) and is below the assumed limit. The resulting RF parameters of the elaborated 2-gap and 3-gap cavity designs are summarized in Table 2.

A higher number of gaps may lead to an increased overall capacitance, which gives more freedom for optimization of the accelerating gaps geometry, where the peak surface electric field is located. An increased capacitance facilitates frequency tuning, while optimizing the spokes geometry towards the low peak surface magnetic field. As a result, the 3-gap Spoke has a more uniform surface field distribution and consequently a lower surface peak field (Table 2).

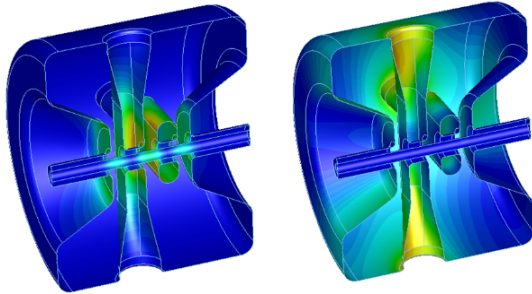


Figure 3: Simulated surface electric (left) and magnetic (right) fields in a 3-gap Spoke cavity; the field strength increases from blue to orange.

Table 2: Comparison of the main RF parameters of the 2-gap and 3-gap cavity

| Parameter | 2-Gap Spoke | 3-Gap Spoke |
|----------------------------------|-------------|-------------|
| E_p/E_{acc} ($\beta\lambda$) | 6.5 | 5.3 |
| B_p/E_{acc} , [mT/(MV/m)] | 9.5 | 7.5 |
| G , [Ω] | 45 | 45 |
| Ra/Q , [Ω] | 114 | 172 |

In Fig. 4 the accelerating gradient distribution along the beam axis of the 3-gap cavity is depicted. The accelerating gradient in the end-cells amounts 60% of the gradient at the cavity centre.

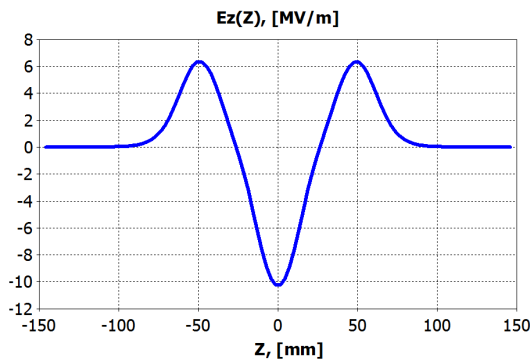


Figure 4: Accelerating field distribution along the beam axis of the 3-gap Spoke cavity.

MECHANICAL DESIGN AND THERMAL PROPERTIES

The geometry of the 3-gap cavity was optimized for advanced mechanical stability in order to minimize affections of Lorentz force detuning and liquid helium pressure instabilities. Several types of stiffening ribs could strengthen the construction against detuning forces as shown in [15-17].

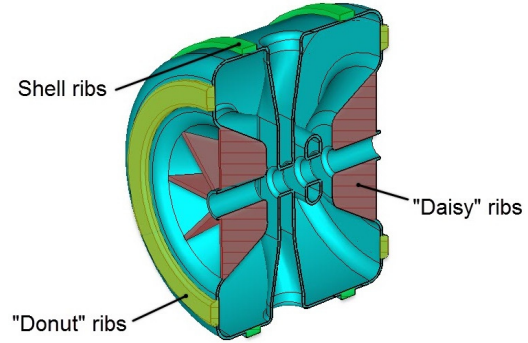


Figure 5: Cross section of the 3-gap Spoke structure; stiffening ribs are highlighted.

For the 3-gap Spoke three types of stiffening ribs have been considered (Fig. 5). Donut-like and shell ribs [15] potentially stiffer the cavity against cool down deformations; daisy-like ribs could maximize the cavity resistance against Lorentz forces and external pressure fluctuations.

All parameters listed below have been calculated for cavities fixed on beam port ends. Fig. 6 shows different configurations of the stiffening ribs, considered during the optimization process.

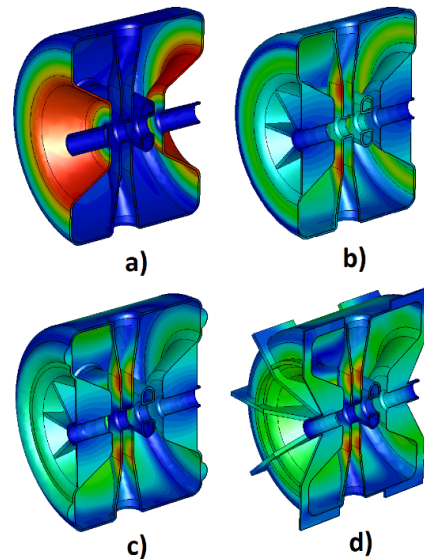


Figure 6: Displacements (mm) under an additional pressure of 1 Bar for the different cavity stiffening options (see Table 3): no ribs (a), "Daisy" ribs (b), "Daisy" and "Donut" ribs (c), all types of ribs (d). The red colour corresponds to a maximum displacement of 0.3 mm (a) and 0.03 mm (b - d).

This is a preprint — the final version is published with IOP

Content from this work may be used under the terms of the CC BY 3.0 licence (© 2018). Any distribution of this work must maintain attribution to the author(s), title of the work, publisher, and DOI.

Content from this work may be used under the terms of the CC BY 3.0 licence (© 2018). Any distribution of this work must maintain attribution to the author(s), title of the work, publisher, and DOI.

Following the comparison of the results, presented in Table 3, an implementation of the “Daisy” ribs significantly strengthened the cavity against all kinds of deformations. However, additionally mounted “Donut” ribs do have an opposite effect and slightly reduce the resistance against external pressure, while different configurations of the shell ribs do not affect the mechanical stability. The use of extended “Daisy” ribs (Fig. 6(d)) turned out to be unnecessary, as they do not improve the mechanical properties of the structure.

Table 3: Comparison of the Mechanical Parameters of Stiffening Configurations (Fig. 6)

| Parameter | a) | b) | c) | d) |
|---|------|------|------|------|
| Frequency sensitivity df/dp , [Hz/mbar] | 257 | 25 | 34 | 31 |
| Frequency offset (4.2 K cooling), [MHz] | 3.00 | 0.87 | 0.85 | 0.84 |
| Detuning coefficient (Lorentz force), [Hz/(MV/m) ²] | 78.6 | 53.1 | 49.7 | 49.3 |

As a result, simulations were carried out applying eight daisy-like ribs for the 3-gap as well as for the 2-gap cavity stiffening. Table 4 shows a comparison of mechanical properties of shells with different stiffening ribs.

As a consequence, the 3-gap cavity is as stiff as the 2-gap cavity. The cross-shaped position of the two spokes strengthens the central part of the resonator, resulting in an improved overall mechanical stability.

Table 4: Comparison of Mechanical Parameters for the 2-gap and 3-gap Constructions.

| Parameter | 2-Gap Spoke | 3-Gap Spoke |
|---|-------------|-------------|
| Frequency sensitivity df/dp , [Hz/mbar] | 59 | 31 |
| Frequency offset (4.2 K cooling), [MHz] | 2 | 0.85 |
| Detuning coefficient (Lorentz force), [Hz/(MV/m) ²] | - | 53.1 |

The Lorentz force detuning coefficient for both structures is relatively high, caused by relatively short accelerating gaps determined by the low particle velocity. Nevertheless, these values correspond to about 1 kHz detuning range at the operating level of the accelerating gradient, which does not exceed the range of the fast tuning system.

CONCLUSION

Different RF- and the mechanical-design of the superconducting spoke re-buncher cavities, to be integrated in the CW-Linac cryomodules at GSI, have been compared. Ultimately, the comparison shows, that both options have their own strengths and weaknesses.

The presented results for an optimized buncher (or few gap cavity) design could be useful for other accelerating projects, which implement superconducting technology for an improving of machine performance, also by an increased (but safe) accelerating gradients [18-24].

However, for the given technical constraints both designs of the buncher show advanced RF and mechanical properties, matching properly the needs of the proposed CW-Linac, which is well in line with other SC accelerator projects.

The obtained simulations show that 3-gap cavities have advantages in electrodynamic properties, as well as these cavities strongly withstand the helium pressure fluctuations; the frequency shift caused by Lorentz force detuning is also limited. Although a 2-gap cavity facilitates the implementation of the power coupler and the already developed fast tuning system into this resonator.

Due to these reasons, the fabrication of a 2-gap re-buncher will be started at once.

REFERENCES

- [1] W. Barth *et al.*, “Upgrade program of the high current heavy ion UNILAC as injector for FAIR”, *Nucl. Instrum. Methods Phys. Res., Sect. A* 577, 211 (2007).
- [2] A. Adonin *et al.*, “Beam brilliance investigation of high current ion beams at GSI heavy ion accelerator facility”, *Rev. Sci. Instrum.* 85, 02A727 (2014).
- [3] W. Barth *et al.*, “U²⁸⁺-intensity record applying a H₂-gas stripper cell”, *Phys. Rev. ST Accel. Beams* 18, 040101 (2015).
- [4] W. Barth *et al.*, “Heavy ion linac as a high current proton beam injector”, *Phys. Rev. ST Accel. Beams* 18, 050102 (2015).
- [5] L. Groening *et al.*, “Benchmarking of measurement and simulation of transverse rms-emittance growth”, *Phys. Rev. ST Accel. Beams* 11, 094201 (2008).
- [6] W. Barth *et al.*, “High brilliance uranium beams for the GSI FAIR”, *Phys. Rev. ST Accel. Beams* 20, 050101 (2017).
- [7] F. Dziuba *et al.*, First cold tests of the superconducting cw demonstrator at GSI, in Proceedings of RuPAC’16, St. Petersburg, Russia (2016), pp. 84–86.
- [8] W. Barth, *et al.*, “EPJ Web of Conferences”, Volume 138, Article number 01026, (2017), DOI: 10.1051/epjconf/201713801026
- [9] M. Schwarz *et al.*, “Beam Dynamics for the sc cw heavy ion Linac at GSI”, Proceedings of IPAC’15, Richmond, VA, USA, p. 3742-3744 (2015).
- [10] W. Barth, K. Aulenbacher, M. Basten *et al.*, “First heavy ion beam tests with a superconducting multigap CH cavity”, *PHYS. REV. ACCEL. BEAMS* 21, 020102 (2018)
- [11] M. Schwarz, M. Basten, M. Busch *et al.*, “Further steps towards the superconducting CW-linac for heavy ions at GSI”, Proceedings of IPAC’16, Busan, South Korea, pp. 896-898 (2016)
- [12] W.Barth *et al.*, “Superconducting CH-Cavity Heavy Ion Beam Testing at GSI, presented at IPAC’18 Conference”, Vancouver, Canada (2018), paper ID:2786
- [13] M. Gusarova, M. Busch, W. A. Barth *et al.*, “DESIGN OF THE TWO-GAP SUPERCONDUCTING RE-BUNCHER”, Proceedings of IPAC’18, this conference.
- [14] H. Padamsee, J. Knobloch, T. Hays “Medium- and Low-β Cavities” in *RF Superconductivity for Accelerators*, Ed. New York, NY, USA: Wiley, 2008, pp. 233.

- [15] G. Lanfranco, G. Apollinari, I. Gonin, T. Khabiboulline, F. McConologue, G. Romanov, R. Wagner. “Design of 325 MHz Single and Triple Spoke Resonators at FNAL”, DOI: 10.1109/TASC.2007.897303
- [16] M. H. Awida, D. Passarelli, P. Berrutti et al., “Development of Low β Single Spoke Resonators for the Front End of the Proton Improvement Plan-II at Fermilab”, DOI: 10.1109/TNS.2017.2737560
- [17] F. L. Krawczyk, R. Garnett, R.P. LaFave et al., “DESIGN OF A LOW- β , 2-GAP SPOKE RESONATOR FOR THE AAA PROJECT”, Proceedings of PAC2001, Chicago, Illinois, USA, submitted for publication.
- [18] A. V. Butenko et al., “Development of NICA injection complex”, in Proceedings of IPAC’14, Dresden, Germany (2014), pp. 2103–2105.
- [19] R. Laxdal, “Recent progress in the superconducting RF Program at TRIUMF/ISAC”, Physica (Amsterdam) 441C, 13 (2006).
- [20] A. E. Aksentev et al., “Conceptual Development of a 600–1000 MeV Proton Beam Accelerator-Driver with Average Beam Power >1 MW”, Atomic Energy Volume 117, Issue 4, pp 270–277 (2015).
- [21] N. Solyak et al., “The concept design of the CW linac of the Project X”, in Proceedings of the IPAC’10, Kyoto, Japan (ICR, Kyoto, 2010), pp. 654–656.
- [22] Gusarova, M.A. et. al., “Research and design of a new RFQ injector for modernization of the LU-20 drift-tube linac(Article)”, Physics of Particles and Nuclei Letters Volume 13, Issue 7, 1 December 2016, pp. 915-918
- [23] Aliev, K.A. et. al., “On application of superconducting resonators for reconstruction of proton injector for nucletron complex”, Physics of Particles and Nuclei Letters Volume 13, Issue 7, 1 December 2016, pp. 911-914
- [24] Aliev, K.A. et. al., “Study of superconducting accelerating structures for megawatt proton driver linac”, Proc. of RuPAC 2014; Obninsk; Russia pp. 318-320